Topological Phases without Crystalline Counterparts

Varjas, Dániel; Lau, Alexander; Pöyhönen, Kim; Akhmerov, Anton R.; Pikulin, Dmitry I.; Fulga, Ion Cosma

DOI
10.1103/PhysRevLett.123.196401

Publication date
2019

Document Version
Final published version

Published in
Physical Review Letters

Citation (APA)
Varjas, D., Lau, A., Pöyhönen, K., Akhmerov, A. R., Pikulin, D. I., & Fulga, I. C. (2019). Topological Phases without Crystalline Counterparts. *Physical Review Letters*, *123*(19), Article 196401. https://doi.org/10.1103/PhysRevLett.123.196401

Topological Phases without Crystalline Counterparts

Dániel Varjas,[1,2,*] Alexander Lau,[2] Kim Pöyhönen,[1,2] Anton R. Akhmerov,[2]
Dmitry I. Pikulin,[3] and Ion Cosma Fulga[4]

[1] *QuTech, Delft University of Technology, P.O. Box 4056, 2600 GA Delft, Netherlands*
[2] *Kavli Institute of Nanoscience, Delft University of Technology, P.O. Box 4056, 2600 GA Delft, Netherlands*
[3] *Microsoft Quantum, Microsoft Station Q, University of California, Santa Barbara, California 93106-6105, USA*
[4] *IFW Dresden and Würzburg-Dresden Cluster of Excellence ct.qmat, Helmholtzstrasse 20, 01069 Dresden, Germany*

(Received 17 May 2019; published 7 November 2019)

We construct a two-dimensional higher-order topological phase protected by a quasicrystalline eightfold rotation symmetry. Our tight-binding model describes a superconductor on the Ammann-Beenker tiling hosting localized Majorana zero modes at the corners of an octagonal sample. In order to analyze this model, we introduce Hamiltonians generated by a local rule, and use this concept to identify the bulk topological properties. We find a $\mathbb{Z}_2$ bulk topological invariant protecting the corner modes. Our work establishes that there exist topological phases protected by symmetries impossible in a crystal.

DOI: 10.1103/PhysRevLett.123.196401

Introduction.—All topological phases known to date can exist in crystalline systems. Strong topological insulators (TI) occur in crystals [1,2], in quasicrystals [3–9], and even in amorphous systems [10–12], and show gapless modes on any boundary, as a consequence of the topologically nontrivial gapped bulk. Weak topological insulators and topological crystalline insulators, on the other hand, rely on crystal symmetries [13–17]. Their gapless topological states appear only on boundaries preserving, at least on average, a subset of lattice symmetries [18,19].

In contrast, in higher-order topological insulators (HOTI) both the bulk and the boundaries are gapped. Instead, the protected gapless modes form at the intersections of two or more boundaries—the corners and hinges of a crystal [20–26]. Unlike in topological crystalline insulators, the corners or hinges may break the lattice symmetry responsible for protecting the HOTI. In those cases, the protection of the boundary modes relies on a discrete symmetry of the entire finite-sized sample. Examples of HOTIs enabled by global symmetries include a three-dimensional (3D) TI placed in a magnetic field [27], hosting chiral hinge modes protected by inversion symmetry, as well as elemental bismuth [28], with helical hinge modes protected by time-reversal symmetry, threefold rotation, and inversion.

Since the set of allowed crystal symmetries is known, it is possible to list all weak, crystalline, and higher-order topological insulators that appear in a crystal. This program has been carried out throughout the past decade, starting with the effect of single symmetries such as mirror or inversion, followed by considering the effect of any order-two symmetry [29,30]. Today, the topological classification spans all known nonmagnetic crystalline compounds [31–33]. Furthermore, the possible band topologies of free fermions have been listed for all 528 two-dimensional and 1651 3D magnetic space groups [34].

In this work, we explore a new class of topological phases by constructing a HOTI phase that is incompatible with a crystalline symmetry, and was therefore overlooked in the previous works. This topological phase relies on the combination of an eightfold rotation and an in-plane reflection. Its hallmark signature is the presence of eight Majorana zero modes bound to the corners of a finite-sized octagonal sample. These modes are robust against any symmetry-preserving perturbation, provided the bulk remains gapped. Because eightfold rotations are forbidden in two dimensions by the crystallographic restriction theorem, the resulting phase has no crystalline counterpart. We propose a modified notion of symmetry protection of HOTI phases applicable to locally generated quasiperiodic Hamiltonians. Using this, we show that the protection of the corner modes does not rely on global symmetry of the sample. We pin down the nontrivial nature of this phase by studying zero modes at topological defects and identifying a bulk topological invariant that determines the formation of Majorana corner modes.

Model.—Our starting point is a tight-binding model describing a pair of oppositely spin-polarized $p \pm ip$ topological superconductors in class D [35]. The real-space Bogoliubov–de–Gennes Hamiltonian is obtained by associating sites and hoppings to the vertexes and edges of an eightfold symmetric Ammann-Beenker tiling [36,37] (see Fig. 1):

$$\mathcal{H} = \sum_j \mathbf{\Psi}_j^\dagger \mathcal{H}_j \mathbf{\Psi}_j + \sum_{\langle j,k\rangle} \mathbf{\Psi}_j^\dagger \mathcal{H}_{jk} \mathbf{\Psi}_k, \tag{1}$$

with $\mathbf{\Psi}_j^\dagger = (\psi_{j,\uparrow}^\dagger, \psi_{j,\uparrow}, \psi_{j,\downarrow}^\dagger, \psi_{j,\downarrow})$, $\psi_{j,\sigma}^\dagger$ the fermionic creation operator for a particle on site j with spin σ, and

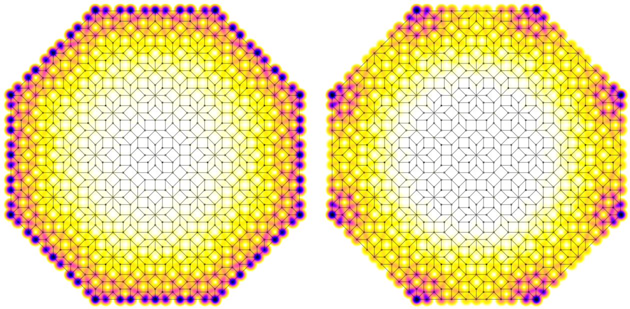

FIG. 1. We define a tight-binding model on an eightfold symmetric patch of the Ammann-Beenker tiling by associating a site to each vertex and a hopping to each of the edges that connect neighboring vertices. Both panels show the real-space distributions of the wave function amplitudes in the eight lowest energy states of the model defined in Eqs. (1) and (5) for $\Delta = t = 1$ and $\mu = -1.7$. Darker colors denote larger amplitudes. For $V = 0$ (left), the system hosts counterpropagating Majorana modes on any edge, protected by mirror symmetry. Setting $V = 1$ (right) gaps out the edge, leading to a HOTI phase. A single Majorana zero mode is localized to each of the eight corners of the tiling.

with $\langle\cdots\rangle$ denoting sites connected by a bond (see Fig. 1). The on-site Hamiltonian is

$$\mathcal{H}_j = \mu\sigma_z\tau_z, \tag{2}$$

where μ is the chemical potential, and Pauli matrices τ and σ act on the electron-hole and spin degrees of freedom, respectively. The hopping terms have the form

$$\mathcal{H}_{jk} = \frac{t}{2}\sigma_z\tau_z + \frac{\Delta}{2i}[\cos(\alpha_{jk})\sigma_z\tau_x + \sin(\alpha_{jk})\sigma_z\tau_y], \tag{3}$$

where t is the normal hopping strength, Δ is the p-wave pairing strength, and α_{jk} is the angle formed by the hopping with respect to the horizontal direction.

The system obeys particle-hole symmetry (PHS), $\{\mathcal{H},\mathcal{P}\} = 0$, with an antiunitary operator $\mathcal{P} = \tau_x\sigma_0\mathbb{1}\mathcal{K}$, where $\mathcal{K}$ denotes complex conjugation and 1 is the identity operator in the space spanned by the sites of the tiling. In addition, Eq. (1) has an in-plane mirror symmetry, $[\mathcal{H}, M] = 0$, with $M = \tau_0\sigma_z\mathbb{1}$. Moreover, due to the shape of the tiling, the finite-sized model obeys a global eightfold rotation symmetry about its center, $[\mathcal{H}, C_8] = 0$. The rotation operator is

$$C_8 = \exp\left(-i\frac{\pi}{8}\sigma_0\tau_z\right)\mathcal{R}, \tag{4}$$

where $\mathcal{R}$ is an orthogonal matrix permuting the sites of the tiling to rotate the whole system by an angle of $\pi/4$.

For $t = \Delta = 1$ and $\mu = -1.7$, the model describes a bilayer system of two 2D class D topological superconductors with opposite Chern numbers, hosting a pair of counterpropagating Majorana edge modes on its boundary (see Fig. 1). The edge modes are prevented from gapping out by the in-plane reflection symmetry. To obtain a HOTI, we introduce a perturbation that breaks both the reflection and rotation symmetries, but preserves their product C_8M. We modify the hoppings by adding the term

$$\mathcal{V} = \sum_{\langle j,k\rangle}\mathbf{\Psi}_j^\dagger\mathcal{V}_{jk}\mathbf{\Psi}_k, \qquad \mathcal{V}_{jk} = \frac{V}{2}\sigma_y\tau_0\cos(4\alpha_{jk}). \tag{5}$$

It anticommutes with the reflection symmetry, $\{\mathcal{V}, M\} = 0$, and opens a gap in the edge spectrum. However, it also anticommutes with the eightfold rotation, such that the gap of the edge states changes sign a total of eight times across the perimeter of the system. This results in the formation of eight Majorana zero modes, as shown in Fig. 1. These modes are localized at the corners of the octagonal sample and are separated from all other states by an energy gap.

Protected corner modes.—Majorana zero modes bound to the corners of the octagonal tiling are a manifestation of the nontrivial bulk topology of the HOTI. As long as the tiling obeys PHS and the global C_8M constraint, the gapless corner states cannot be removed by any perturbation restricted to the system boundary. There is an intuitive explanation for this (see also Ref. [22]): the minimal surface manipulation compatible with PHS and C_8M consists of gluing a Kitaev chain onto each of the eight edges of the tiling, such that adjacent chains are mapped onto each other under C_8M. This process changes the number of corner Majoranas by an even number and the original zero modes cannot gap out. This suggests that the octagonal HOTI has a $\mathbb{Z}_2$ classification.

To verify that the corner states are not merely an artifact of an exact C_8M symmetry of the entire sample, we also consider asymmetric cutouts of the quasicrystal. The quasiperiodicity of a quasicrystal implies that any finite region of an infinite sample repeats infinitely many times [4]. Hence, there are infinitely many locations in the quasicrystal that look identical to the vicinity of a corner of an exactly eightfold symmetric sample at a scale much larger than the extent of the bound state. By the locality of the Hamiltonian, such a corner (in either a semi-infinite system or an asymmetric finite sample) will also host a Majorana zero mode, as illustrated in Fig. 2(a). These zero modes are "extrinsic" [25], as there is no exact symmetry relating the two edges emanating from such a corner. This implies that, analogous to crystalline HOTIs, attaching a Kitaev wire to one of the edges but not to the other does not break any symmetries and the zero mode can, in principle, be gapped out by an edge perturbation.

Therefore, we impose the physical restriction of *quasiperiodicity* on the Hamiltonians we consider in the following. We demand that the Hamiltonian is generated by a local, eightfold symmetric rule: every term is determined by the quasicrystal configuration in a finite radius

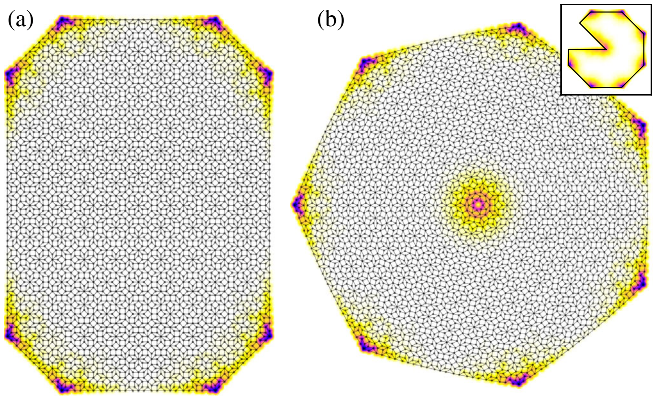

FIG. 2. Wave function amplitudes of eight zero modes in various finite geometries. (a) Asymmetric sample with corners locally identical to corners of a symmetric sample. (b) Sample with a C_8M defect. Away from the defect at the center, the system is locally identical to the original model. Inset: Sample with one octant cut out, but without gluing together the two sides of the cut.

environment, in a symmetric fashion. The quasiperiodicity of the tiling means that the semi-infinite edges emanating from an approximately symmetric corner, while not exact symmetry images, are indistinguishable by only inspecting finite regions. This prevents a deformation of the Hamiltonian that produces a gapped Kitaev chain on only one of these edges, resulting in protected corner modes.

Disclination modes.—We now prove that the phase discussed above is indeed a *bulk* topological phase protected by C_8M symmetry by showing that pointlike fluxes (topological defects) of this symmetry capture a Majorana zero mode [38,39]. The C_8M flux is inserted into the system by the following procedure (similar to Ref. [40]): first, we take a large eightfold symmetric sample and cut out one octant bordered by a cut $\mathcal{C}$, connecting the center of the tiling with the boundary, and by its symmetry image $C_8\mathcal{C}$ [see inset of Fig. 2(b)]. Then, we glue the two sides of the cut back together by identifying sites on the two sides of the cut related by C_8M symmetry. The hoppings across the cut are $\mathcal{H}_{C_8 j,k} = U_{C_8M}\mathcal{H}_{j,k}$, where $C_8 j$ is the C_8 image of site j and U_{C_8M} is the on-site unitary action of the C_8M symmetry. The cut $\mathcal{C}$, similar to a Dirac string, is not detectable locally. Indeed, applying a basis transformation U_{C_8M} to a single site neighboring the cut (and identity elsewhere) moves the site to the other side of the cut. This makes the location of the cut basis dependent and locally indistinguishable from the bulk with no cut, with the exception of the center of the system where the cut terminates.

As illustrated in Fig. 2(b), the resulting sample has eight Majorana zero modes: seven at the corners and one at the disclination core. The disclination mode cannot be removed without closing the bulk gap, proving that the HOTI phase is separated from the trivial phase by a bulk phase transition.

Bulk topological invariant.—We now develop an invariant that characterizes the bulk topology of the quasicrystalline system. For this purpose, we consider the momentum-dependent effective Hamiltonian $H_{\mathrm{eff}} = G_{\mathrm{eff}}^{-1}$, defined through the projection of the single-particle Green's function onto plane-wave states:

$$G_{\mathrm{eff}}(k)_{n,m} = \langle k, n|G|k, m\rangle, \tag{6}$$

where $|k, n\rangle$ is a normalized plane-wave state with nonzero amplitude only in the local orbital n, and $G = \lim_{\eta\to 0}(H + i\eta)^{-1}$ is the zero-energy Green's function of the full Hamiltonian (see Supplemental Material [41]).

An important property of H_{eff} is that its gap closes only when the gap of the full Hamiltonian closes. We are going to use this to construct topological invariants: if an invariant defined in terms of H_{eff} can only change when the gap in H_{eff} closes, it implies a bulk phase transition of the full Hamiltonian. The classification we derive below is thus a subset of the full topological classification of C_8M symmetric systems.

To define the topological invariant we inspect the symmetry representations of C_8M and $\mathcal{P}$ acting on H_{eff} at the C_8-invariant momentum $k = 0$ [38]. The eigenvalues of C_8M have the form $\omega_n = \exp[i(\pi/8)n]$, with $n = [\pm1, \pm3, \pm5, \pm7]$, and eigenstates $|n\rangle$ and $-n\rangle$ are related by $\mathcal{P}$. By restricting $H_{\mathrm{eff}}(k = 0)$ to C_8M eigensubspaces of $\omega_{\pm n}$, we calculate the zero-dimensional class D invariant of each block, which is the sign of the Pfaffian in the Majorana basis. This yields $\nu_{n,k=0} = \pm1$, for $n \in [1, 3, 5, 7]$, resulting in a $\mathbb{Z}_2^4$ classification. In our model, $H_{\mathrm{eff}}(k = 0)$ has two invariant blocks corresponding to pairs of $n = \pm1$ and ±7, respectively, while there are no states in the local Hilbert space corresponding to the other C_8M eigenstates with $n = \pm3, \pm5$. We find that $H_{\mathrm{eff}}(k = 0)$ goes through a band inversion at $\mu \approx -2$ when both Pfaffians switch sign. This, however, cannot be a stable topological invariant, as it also distinguishes different atomic insulators with on-site Hamiltonians of opposite sign and vanishing hoppings.

To provide an invariant that is insensitive to addition of atomic insulators, we invoke the cut-and-project method generating the 2D Ammann-Beenker tiling from a four-dimensional cubic lattice (see Ref. [4] and Supplemental Material [41]). Plane-wave states in the 4D Brillouin zone provide a complete basis for all states on the 4D lattice, and an overcomplete basis for the quasicrystal. Some of these plane waves cannot be exactly represented by purely 2D plane waves, but can be approximated by those to arbitrary precision. We call these patterns of complex phases on the quasicrystal generalized plane waves. The generalized plane waves important for the topological invariant are the ones at 4D momenta invariant under C_8 modulo reciprocal lattice vectors. Those are $\Gamma = (0, 0, 0, 0) \equiv 0$, which we have already discussed above, and $\Pi = (\pi, \pi, \pi, \pi)$. The latter produces alternating $\pm$ signs on nearest-neighbor sites

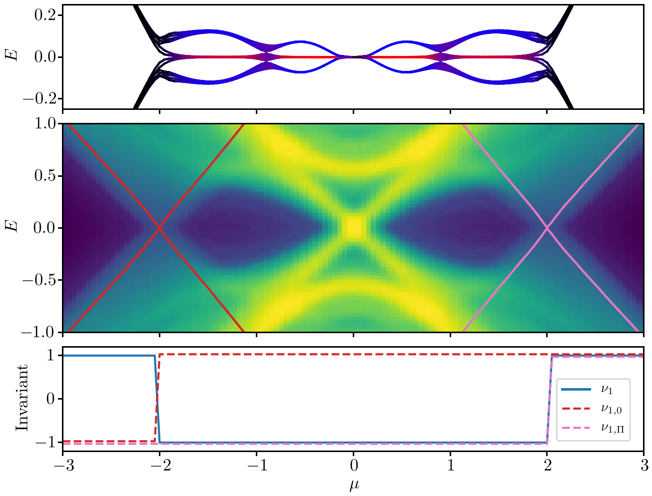

FIG. 3. Topological phase transitions in the quasicrystal HOTI model as a function of chemical potential μ with $t = 1$, $\Delta = 2$, and $V = 1.5$. Top: Spectrum of the 24 states closest to zero energy in a finite sample. The line color shows the weight of the state on the corners (red), edges (blue), and bulk (black). The bulk gap closes at $\mu \approx \pm 2$, delimiting the phase with eight Majorana corner modes. The edge gap closes at $\mu \approx \pm 0.9$ and the bulk gap closes around $\mu = 0$ without affecting the topological properties. Middle: Evolution of the bulk density of states, with lighter colors denoting larger densities. Overlaid is the spectrum of the effective Hamiltonian at $k = 0$ (red) and $k = \Pi$ (pink). Bottom: Topological invariants $\nu_{1,0}$, $\nu_{1,\Pi}$ and $\nu_1 = \nu_{1,0}/\nu_{1,\Pi}$.

of the quasicrystal. Looking at the symmetry representation of $H_{\mathrm{eff}}(k = \Pi)$, we find a band inversion at $\mu \approx 2$, which is similar to the one of $H_{\mathrm{eff}}(k = 0)$ at $\mu \approx -2$. As a consequence, $\nu_{n,0} = -\nu_{n,\Pi}$ for $n \in [1, 7]$ in the range $-2 \lesssim \mu \lesssim 2$. Stable $\mathbb{Z}_2$ invariants are therefore defined by $\nu_n = \nu_{n,0}/\nu_{n,\Pi}$.

In the atomic limit, we have $\nu_n = 1$. Thus, the nontrivial value signals an obstructed atomic limit. Moreover, we find that phases with both gapped bulk and gapped edges have only two independent invariants, since $\nu_1 = \nu_7$ and $\nu_3 = \nu_5$ (see Supplemental Material [41]). In the topological phase, our model has $\nu_1 = \nu_7 = -1$ and $\nu_3 = \nu_5 = +1$, as illustrated in Fig. 3. The $\mathbb{Z}_2$ invariant characterizing the presence of corner Majoranas is the product $\nu_1\nu_3$, while the corner modes do not distinguish between other phases in the richer $\mathbb{Z}_2^2$ bulk classification.

Discussion.—We have demonstrated the existence of a quasicrystalline higher-order topological phase. The topological protection of this phase explicitly requires broken translation symmetry, since it is protected by a point group symmetry incompatible with any periodic crystal structure in two or three dimensions. In the nontrivial phase, both the bulk and the edges are gapped, whereas eight Majorana zero modes are bound to the corners of the octagonal tiling. These modes are associated with a nontrivial bulk invariant and are robust against symmetry-preserving perturbations that do not close the bulk gap.

While we have treated the special case of a class D topological superconductor with C_8M symmetry, the ideas we have presented generalize to a wider range of systems. It should be possible to extend our work to other symmetry classes, other point group symmetries, and higher dimensions. We note, however, that the basic line of argument we used to construct the model, reliant on an alternating sign of the mass term at the boundary, does not work for odd rotations, e.g., C_5. For this, it would be necessary to introduce topological protection in another manner.

Our investigation opens several directions for future work. First, while we have shown a single example as a proof of principle, the range of possible, purely aperiodic topological insulators and semimetals remains unknown. Furthermore, it is also unclear which tools would be required to characterize all such systems in practice, as most existing methods for obtaining topological invariants in the presence of point group symmetries explicitly rely on momentum space. We have presented one possible approach applicable to translation-symmetry breaking systems. One might also consider real-space topological invariants, similar to the ones defined for finite systems with boundaries, as done in Ref. [47] for strong topological insulators. Another interesting direction to explore would be to consider classes of quasicrystals obtained by a cut-and-project method from a higher-dimensional periodic lattice, such as the one we used here, and attempt a topological classification via dimensional reduction. The results of this approach will, however, be limited, since there are quasicrystals not obtainable by such a method. Lastly, the new methods explored here are applicable to crystalline systems as well. To show that we found a bulk topological phase, we introduced the notion of a quasi-periodic Hamiltonian, where terms are only sensitive to the quasicrystal configuration in a finite radius environment. This notion of locality also applies to crystalline, disordered, and amorphous materials, promising a new direction to establish the topological protection of "extrinsic" corner modes via bulk invariants.

Finally, there is the question of how such a topological phase may be observed experimentally. While we can predict that this C_8M protected phase will never be realized in any crystalline system, it may be possible to obtain eightfold symmetry protected corner modes in the recently discovered superconducting quasicrystals [48,49]. Alternatively, one may consider a variety of so-called "topological simulators," including ultracold atoms [50–52], photonic crystals [53,54], coupled electronic circuit elements (called topolectric circuits [55]), as well as acoustic and mechanical metamaterials [56,57]. These systems allow for a site connectivity bypassing the chemical constraints inherent in crystal growth processes, and have been successfully used to demonstrate both higher-order topological phases [58–60] as well as topologically nontrivial quasicrystals [61,62].

The data shown in the figures as well as the code generating all of the data are available in Ref. [63].

We thank Ulrike Nietsche for technical assistance. We are grateful to P. Perez-Piskunow for helpful discussions about the kernel polynomial method (KPM) and the use of his KPM Green's function code. We thank P. Perez-Piskunow and M. Fruchart for sharing the KPM-based method to calculate the Chern number in disordered systems [64]. We thank B. Roy and V. Juricic for discussions about Ref. [65], a manuscript which motivated this project. This work was supported by the DFG through the Würzburg-Dresden Cluster of Excellence on Complexity and Topology in Quantum Matter–*ct.qmat* (EXC 2147, Project No. 39085490). This work was supported by ERC Starting Grant No. 638760, NWO VIDI Grant No. 680-47-53, the U.S. Office of Naval Research, and through the subsidy for top consortia for knowledge and innovation (TKl toeslag) by the Dutch ministry of economic affairs.

I. C. F. constructed the model used in the Letter, initiated, and oversaw the project. All authors took part in an extensive survey of topological invariants to characterize the system. D. V. conceived and carried out the analysis based on topological defects and bulk topological invariants. I. C. F. and D. V. performed the numerical calculations, and D. V. and A. R. A. produced the figures in the Letter. All authors took part in formulating the results and writing the Letter.

*dvarjas@gmail.com

[1] M. Z. Hasan and C. L. Kane, Colloquium: Topological insulators, Rev. Mod. Phys. **82**, 3045 (2010).
[2] X.-L. Qi and S.-C. Zhang, Topological insulators and superconductors, Rev. Mod. Phys. **83**, 1057 (2011).
[3] D. Shechtman, I. Blech, D. Gratias, and J. W. Cahn, Metallic Phase with Long-Range Orientational Order and No Translational Symmetry, Phys. Rev. Lett. **53**, 1951 (1984).
[4] M. Baake and U. Grimm, *Aperiodic Order. A Mathematical Invitation* (Cambridge University Press, Cambridge, England, 2013), Vol. 1.
[5] M. Zoorob, M. Charlton, G. Parker, J. Baumberg, and M. Netti, Complete photonic bandgaps in 12-fold symmetric quasicrystals, Nature (London) **404**, 740 (2000).
[6] W. Steurer and D. Sutter-Widmer, Photonic and phononic quasicrystals, J. Phys. D **40**, R229 (2007).
[7] Y. E. Kraus, Y. Lahini, Z. Ringel, M. Verbin, and O. Zilberberg, Topological States and Adiabatic Pumping in Quasicrystals, Phys. Rev. Lett. **109**, 106402 (2012).
[8] M. Verbin, O. Zilberberg, Y. E. Kraus, Y. Lahini, and Y. Silberberg, Observation of Topological Phase Transitions in Photonic Quasicrystals, Phys. Rev. Lett. **110**, 076403 (2013).
[9] I. C. Fulga, D. I. Pikulin, and T. A. Loring, Aperiodic Weak Topological Superconductors, Phys. Rev. Lett. **116**, 257002 (2016).
[10] I. C. Fulga, B. van Heck, J. M. Edge, and A. R. Akhmerov, Statistical topological insulators, Phys. Rev. B **89**, 155424 (2014).
[11] A. Agarwala and V. B. Shenoy, Topological Insulators in Amorphous Systems, Phys. Rev. Lett. **118**, 236402 (2017).
[12] K. Pöyhönen, I. Sahlberg, A. Westström, and T. Ojanen, Amorphous topological superconductivity in a Shiba glass, Nat. Commun. **9**, 2103 (2018).
[13] L. Fu, C. L. Kane, and E. J. Mele, Topological Insulators in Three Dimensions, Phys. Rev. Lett. **98**, 106803 (2007).
[14] B. Rasche, A. Isaeva, M. Ruck, S. Borisenko, V. Zabolotnyy, B. Büchner, K. Koepernik, C. Ortix, M. Richter, and J. van den Brink, Stacked topological insulator built from bismuth-based graphene sheet analogues, Nat. Mater. **12**, 422 (2013).
[15] L. Fu, Topological Crystalline Insulators, Phys. Rev. Lett. **106**, 106802 (2011).
[16] T. L. Hughes, E. Prodan, and B. A. Bernevig, Inversion-symmetric topological insulators, Phys. Rev. B **83**, 245132 (2011).
[17] C.-K. Chiu, J. C. Y. Teo, A. P. Schnyder, and S. Ryu, Classification of topological quantum matter with symmetries, Rev. Mod. Phys. **88**, 035005 (2016).
[18] Z. Ringel, Y. E. Kraus, and A. Stern, Strong side of weak topological insulators, Phys. Rev. B **86**, 045102 (2012).
[19] A. Lau, J. van den Brink, and C. Ortix, Topological mirror insulators in one dimension, Phys. Rev. B **94**, 165164 (2016).
[20] W. A. Benalcazar, B. A. Bernevig, and T. L. Hughes, Quantized electric multipole insulators, Science **357**, 61 (2017).
[21] W. A. Benalcazar, B. A. Bernevig, and T. L. Hughes, Electric multipole moments, topological multipole moment pumping, and chiral hinge states in crystalline insulators, Phys. Rev. B **96**, 245115 (2017).
[22] F. Schindler, A. M. Cook, M. G. Vergniory, Z. Wang, S. S. P. Parkin, B. A. Bernevig, and T. Neupert, Higher-order topological insulators, Sci. Adv. **4**, eaat0346 (2018).
[23] L. Trifunovic and P. W. Brouwer, Higher-Order Bulk-Boundary Correspondence for Topological Crystalline Phases, Phys. Rev. X **9**, 011012 (2019).
[24] J. Langbehn, Y. Peng, L. Trifunovic, F. von Oppen, and P. W. Brouwer, Reflection-Symmetric Second-Order Topological Insulators and Superconductors, Phys. Rev. Lett. **119**, 246401 (2017).
[25] M. Geier, L. Trifunovic, M. Hoskam, and P. W. Brouwer, Second-order topological insulators and superconductors with an order-two crystalline symmetry, Phys. Rev. B **97**, 205135 (2018).
[26] S. Franca, J. van den Brink, and I. C. Fulga, An anomalous higher-order topological insulator, Phys. Rev. B **98**, 201114 (R) (2018).
[27] M. Sitte, A. Rosch, E. Altman, and L. Fritz, Topological Insulators in Magnetic Fields: Quantum Hall Effect and Edge Channels with a Nonquantized θ Term, Phys. Rev. Lett. **108**, 126807 (2012).
[28] F. Schindler *et al.*, Higher-order topology in bismuth, Nat. Phys. **14**, 918 (2018).
[29] C.-K. Chiu, H. Yao, and S. Ryu, Classification of topological insulators and superconductors in the presence of reflection symmetry, Phys. Rev. B **88**, 075142 (2013).

[30] K. Shiozaki and M. Sato, Topology of crystalline insulators and superconductors, Phys. Rev. B **90**, 165114 (2014).

[31] J. Kruthoff, J. de Boer, J. van Wezel, C. L. Kane, and R.-J. Slager, Topological Classification of Crystalline Insulators Through Band Structure Combinatorics, Phys. Rev. X **7**, 041069 (2017).

[32] H. C. Po, A. Vishwanath, and H. Watanabe, Symmetry-based indicators of band topology in the 230 space groups, Nat. Commun. **8**, 50 (2017).

[33] B. Bradlyn, L. Elcoro, J. Cano, M. G. Vergniory, Z. Wang, C. Felser, M. I. Aroyo, and B. A. Bernevig, Topological quantum chemistry, Nature (London) **547**, 298 (2017).

[34] H. Watanabe, H. C. Po, and A. Vishwanath, Structure and topology of band structures in the 1651 magnetic space groups, Sci. Adv. **4**, eaat8685 (2018).

[35] N. Read and D. Green, Paired states of fermions in two dimensions with breaking of parity and time-reversal symmetries and the fractional quantum Hall effect, Phys. Rev. B **61**, 10267 (2000).

[36] B. Grünbaum and G. C. Shephard, *Tilings and Patterns* (W. H. Freeman & Co., New York, 1986).

[37] F. Beenker, Eindhoven University of Technology Report, Algebraic theory of non-periodic tilings of the plane by two simple building blocks: A square and a rhombus, 1982.

[38] J. C. Y. Teo and T. L. Hughes, Existence of Majorana-Fermion Bound States on Disclinations and the Classification of Topological Crystalline Superconductors in Two Dimensions, Phys. Rev. Lett. **111**, 047006 (2013).

[39] W. A. Benalcazar, J. C. Y. Teo, and T. L. Hughes, Classification of two-dimensional topological crystalline superconductors and Majorana bound states at disclinations, Phys. Rev. B **89**, 224503 (2014).

[40] M. Geier, A. Lau, and I. C. Fulga (to be published).

[41] See Supplemental Material at http://link.aps.org/supplemental/10.1103/PhysRevLett.123.196401, which includes Refs. [42–46], for details of the quasicrystal construction, effects of edge terminations, calculation of topological invariants, effects of other symmetries, and numerical methods.

[42] C. W. Groth, M. Wimmer, A. R. Akhmerov, and X. Waintal, Kwant: A software package for quantum transport, New J. Phys. **16**, 063065 (2014).

[43] A. Weiße, G. Wellein, A. Alvermann, and H. Fehske, The kernel polynomial method, Rev. Mod. Phys. **78**, 275 (2006).

[44] D. Varjas, T. Ö. Rosdahl, and A. R. Akhmerov, Qsymm: Algorithmic symmetry finding and symmetric Hamiltonian generation, New J. Phys. **20**, 093026 (2018).

[45] R. Bianco and R. Resta, Mapping topological order in coordinate space, Phys. Rev. B **84**, 241106(R) (2011).

[46] M. Wimmer, Algorithm 923: Efficient numerical computation of the Pfaffian for dense and banded skew-symmetric matrices, ACM Trans. Math. Softw. **38**, 1 (2012).

[47] T. A. Loring, *K*-theory and pseudospectra for topological insulators, Ann. Phys. (Amsterdam) **356**, 383 (2015).

[48] K. Kamiya, T. Takeuchi, N. Kabeya, N. Wada, T. Ishimasa, A. Ochiai, K. Deguchi, K. Imura, and N. K. Sato, Discovery of superconductivity in quasicrystal, Nat. Commun. **9**, 154 (2018).

[49] R. N. Araújo and E. C. Andrade, Conventional superconductivity in quasicrystals, Phys. Rev. B **100**, 014510 (2019).

[50] I. Bloch, J. Dalibard, and S. Nascimbène, Quantum simulations with ultracold quantum gases, Nat. Phys. **8**, 267 (2012).

[51] K. Viebahn, M. Sbroscia, E. Carter, J.-C. Yu, and U. Schneider, Matter-Wave Diffraction from a Quasicrystalline Optical Lattice, Phys. Rev. Lett. **122**, 110404 (2019).

[52] T. A. Corcovilos and J. Mittal, Two-dimensional optical quasicrystal potentials for ultracold atom experiments, Appl. Opt. **58**, 2256 (2019).

[53] L. Lu, J. D. Joannopoulos, and M. Soljačić, Topological photonics, Nat. Photonics **8**, 821 (2014).

[54] T. Ozawa *et al.*, Topological photonics, Rev. Mod. Phys. **91**, 015006 (2019).

[55] C. H. Lee, S. Imhof, C. Berger, F. Bayer, J. Brehm, L. W. Molenkamp, T. Kiessling, and R. Thomale, Topolectrical circuits, Commun. Phys. **1**, 39 (2018).

[56] R. Süsstrunk and S. D. Huber, Observation of phononic helical edge states in a mechanical topological insulator, Science **349**, 47 (2015).

[57] L. M. Nash, D. Kleckner, A. Read, V. Vitelli, A. M. Turner, and W. T. M. Irvine, Topological mechanics of gyroscopic metamaterials, Proc. Natl. Acad. Sci. U.S.A. **112**, 14495 (2015).

[58] J. Noh, W. A. Benalcazar, S. Huang, M. J. Collins, K. P. Chen, T. L. Hughes, and M. C. Rechtsman, Topological protection of photonic mid-gap defect modes, Nat. Photonics **12**, 408 (2018).

[59] B.-Y. Xie, H.-F. Wang, H.-X. Wang, X.-Y. Zhu, J.-H. Jiang, M.-H. Lu, and Y.-F. Chen, Second-order photonic topological insulator with corner states, Phys. Rev. B **98**, 205147 (2018).

[60] H. Xue, Y. Yang, F. Gao, Y. Chong, and B. Zhang, Acoustic higher-order topological insulator on a Kagome lattice, Nat. Mater. **18**, 108 (2019).

[61] M. Verbin, O. Zilberberg, Y. E. Kraus, Y. Lahini, and Y. Silberberg, Observation of Topological Phase Transitions in Photonic Quasicrystals, Phys. Rev. Lett. **110**, 076403 (2013).

[62] M. A. Bandres, M. C. Rechtsman, and M. Segev, Topological Photonic Quasicrystals: Fractal Topological Spectrum and Protected Transport, Phys. Rev. X **6**, 011016 (2016).

[63] D. Varjas, A. Lau, K. Pöyhönen, A. R. Akhmerov, D. I. Pikulin, and I. C. Fulga, Topological phases without crystalline counterparts, https://doi.org/10.5281/zenodo.2639407.

[64] D. Varjas, M. Fruchart, A. R. Akhmerov, and P. Perez-Piskunow, Computation of topological invariants of disordered materials using the kernel polynomial method, arXiv:1905.02215.

[65] A. Agarwala, V. Juricic, and B. Roy, Higher order topological insulators in amorphous solids, arXiv:1902.00507.